

Sampling unknown large networks restricted by low sampling rates

Bo Jiao

Email: jiaobleetc@outlook.com

School of Information Science & Technology, Xiamen University Tan Kah Kee College, ZhangZhou, 363123, China

Abstract: Graph sampling plays an important role in data mining for large networks. Specifically, larger networks often correspond to lower sampling rates. Under the situation, traditional traversal-based samplings for large networks usually have an excessive preference for densely-connected network core nodes. Aim at this issue, this paper proposes a sampling method for unknown networks at low sampling rates, called SLSR, which first adopts a random node sampling to evaluate a degree threshold, utilized to distinguish the core from periphery, and the average degree in unknown networks, and then runs a double-layer sampling strategy on the core and periphery. SLSR is simple that results in a high time efficiency, but experimental evaluation confirms that the proposed method can accurately preserve many critical structures of unknown large networks at sampling rates not exceeding 10%.

Key Words: Graph sampling, unknown network, low sampling rate, data mining.

1 Introduction

Graph sampling extracts nodes or edges to create subgraphs representing an original network, which is often used as pre-processing before data mining to reduce the scale of datasets^[1-5] or as post-processing after optimization to represent the original network more accurately^[6-9]. The former usually adopts traversal-based samplings^[5] that simulate walkers travelling on unknown networks based on the neighbor information of the nodes they are accessing. The traversal-based samplings^[5] are time efficient, which enables complex mining algorithms, such as graph convolutional networks^[1], subgraph pattern mining^[2,3] and network embedding^[4], to be applied to networks with more than one million nodes. The latter adopts samplings that construct optimization models^[6-9] to minimize the difference between known original networks and sampled subgraphs. Approximation algorithms used for solving the optimization models are powerful in representing objective structures of the original networks but are time-consuming^[6-9]. This paper focuses on the traversal-based samplings in pre-processing systems that travel on unknown original networks, and intends to represent more important structures of the networks with high time efficiency.

MHRW (Metropolis-Hastings Random Walk)^[10] and SRW (Simple Random Walk)^[11] are two classical traversal-based samplings. Based on Markov chain random models, MHRW is unbiased, which samples each node with uniform stationary distribution, whereas, SRW is biased, that is, the probability of a node being sampled is proportional to its degree^[10,11]. This paper focuses on ubiquitous scale-free networks exhibiting core-periphery structures, which consist of a dense core and a sparse periphery^[12-15]. The core determines many important structures of the networks, such as low-diameter; however, it is almost ignored by unbiased samplings since the number of nodes in

the core is extremely small. On the contrary, biased samplings preserve more structures determined by the core nodes that have high-degrees. However, the above-mentioned node sampling probability of SRW corresponds to the convergence state of Markov chain ^[11].

Sampling rate is defined as the ratio of the number of nodes (or edges) between sampled and original networks ^[5]. Low sampling rates are needed to improve time efficiency on large networks, but also make it difficult to achieve the convergence of Markov chain. In the core-periphery structures of scale-free networks, each core node is well-connected by periphery nodes but the latter are not well-connected to each other ^[12-15], that is, the walkers of biased samplings are more likely to be attracted to the core under constraints of low sampling rates, resulting in loss of structures related to the periphery that occupies the vast majority of nodes in the networks. Thus, this paper proposes a sampling for unknown networks at low sampling rates, called SLSR, objective to achieve a balanced sampling on the core-periphery structures.

The contributions of this paper are as follows: Section 3 investigates the design principles of SLSR. Section 4 provides a random node sampling to evaluate the average degree (AD) and degree threshold (DT) of original unknown large networks. Section 5 designs the traversal-based sampling SLSR under the guidance of AD and DT. Section 6 evaluates SLSR with related methods and verifies that SLSR can capture many critical structures except for degree, including assortativity, path length, clustering, graph spectrum, centrality and communities.

2 Related work

2.1 Graph sampling on unknown networks

Node/edge-based samplings choose a set of nodes (or edges) at random and extract the sub-graphs induced by the chosen nodes (or edges), including uniform samplings, such as random node (RN) and random edge (RE), and non-uniform samplings, such as random degree node (RDN) and random PageRank node (PRN) ^[5,16]. Specifically, nodes can be sampled proportional to the degree centrality by RDN, and proportional to the PageRank weight by PRN ^[5].

Traversal-based samplings start with one or more seeds and crawl on unknown original networks based on the neighbor information of the nodes they are accessing. Forest fire (FF), which is a variant of breadth first (BF) and snow ball (SB), performs superior in time efficiency since each node in the unknown networks is traversed no more than once ^[17]. FF starts by a random seed, then burns a fraction of its neighbors that have not been traversed, where the fraction is randomly drawn from a geometric distribution, and the process is recursively repeated for each burnt neighbor until the desired sample size is obtained ^[5]. Random walk with restart (RWR) is a variant of SRW, which flies back to the starting seed with probability 0.15 and re-start the random walk ^[5]. Leskovec et al. ^[5] showed that both of the biased samplings FF and RWR perform best on scale-free networks in contrast to the above-mentioned node/edge-based samplings. To address the issue of the slow convergence rate of random walk samplings, Li et al. ^[18] proposed a common neighbor aware random walk (CNARW) sampling that is biased towards neighbors with low neighborhood overlap. Rank degree (RD) is a multi-seed sampling ^[19], which adopts a predetermined number of random starting seeds to avoid the sampling trapped locally, then iteratively explores top- k highest-degree neighbors of each seed and adds them to the seed set. In addition, some samplings were designed to capture specific network structures, such as, community structure expansion (CSE) ^[20], sampling social networks using shortest paths (SP) ^[21], and dual random-walk based sampling (DRaWS) that can efficiently estimate distributions of degree and clique size over social networks ^[22].

Stream-based samplings generate subgraphs from activity networks that can be treated as a stream of edges ^[23,24]. In the networks, besides the unknown topology, the node set and the neighbor information of any node are unobtainable. Owing to restrictions on access to the activity networks, representing more structures of the networks is still a challenging task.

2.2 Graph sampling on known networks

If all network information of a dataset is known, complex structures hidden in the dataset can be discovered in advance. Hong et al. ^[6] first extracted precise structures, such as k -core, closeness, betweenness, and eigenvector centrality, from known original networks, and then reduced the scale of the networks under the guidance of the structures. Sampling on known networks helps preserve more precise structures, but usually comes at the cost of time ^[6-9].

3 Problem formulation and design principles

3.1 Problem formulation

This paper focuses on simple, undirected, and scale-free original networks, in which self-loops, multi-edges, direction of edges are ignored. In the original networks, we assume that the topological information is unknown, but the node set and the neighbors of sampled nodes can be accessed ^[5,16-22]. The notions used by our SLSR sampling are listed in Table 1.

Table 1. Notions and descriptions

Notions	Descriptions
$G_{org} = (V_{org}, E_{org})$	An unknown original network G_{org} where V_{org} and E_{org} respectively denote the node set and edge set. Please note that G_{org} is a simple and undirected graph.
\bar{d}_{org}	The average degree of G_{org} , which will be evaluated by a random node sampling.
\ddot{d}_{org}	A degree threshold of G_{org} , which will be evaluated by a random node sampling.
$N_{org}(v)$	The set of neighbor nodes of a sampled node v in G_{org} , which can be obtained by the traversal-based samplings.
$\ \cdot\ $	The cardinality of a set.
$d_{org}(v)$	The degree of a sampled node v in G_{org} , where $d_{org}(v) = \ N_{org}(v)\ $.
$S_1 - S_2$	A set consisting of elements that belong to S_1 but not to S_2 , where S_1 and S_2 denote two sets.
R	A sampling rate.
$G_{sub} = (V_{sub}, E_{sub})$	A sampled subgraph of G_{org} where $V_{sub} \subseteq V_{org}$ and $E_{sub} \subseteq E_{org}$.

3.2 Design principles

The classical Barabasi-Albert (BA) scale-free evolving network model ^[25] confirms that the degree distribution of the network almost remains the same as the scale changes. Please note that the distribution only represents low-degrees of nodes in periphery, ignoring high-degrees of nodes in core, because the number of core nodes is extremely smaller than that of periphery nodes ^[12-15]. Based on the preferential attachment (PA) rule adopted by the BA model ^[25], which attaches each newly-added node preferentially to high-degree nodes, the degrees of core nodes quickly grow with increasing network scale, that is, the larger an original network, the greater the difference in degree between the core and periphery nodes, which causes the biased samplings on large networks to be overly attracted to the core at low sampling rates. The degree distribution is an important metric and the existing biased samplings are good at capturing the metric under specific conditions ^[16-22]. Thus,

the first principle **P1** is to create a core-periphery framework in which the existing biased samplings continue to be used but are only limited to the periphery sampling, that is, the core, which hinders the capture of the degree distribution, is stripped off and processed separately.

During changes in a scale-free network, such as scale-reduction, the core has a low variability^[15]. In addition, based on the fractal characteristic^[25], the communities of the network also represent core-periphery structures^[26]. Specifically, the community cores are mainly located in the core of the network, that is, the network core represents the structure of community centers. Thus, the second principle **P2** is to maximize the preservation of the connections in the network core.

Owing to sparse connections between periphery nodes, faster information exchange between these nodes depends on core nodes^[12-15]. Specifically, based on the PA rule^[25], the higher the degree of a core node, the greater its probability of being connected by other newly-added periphery nodes, that is, the core node has stronger ability to shorten the path length between periphery nodes. Thus, the third principle **P3** is to preserve a proportion of core neighbors with top highest degrees for each sampled periphery node, where the proportion can be determined by the AD of original networks that will be evaluated by a random node sampling in Section 4. Please note that the second and third principles are helpful in preserving the path length distribution.

The periphery is the main contributor of the clustering coefficient distribution since it occupies the vast majority of nodes in the network^[12-15]. Based on the PA rule^[25], the neighbors of a periphery node tend to be located in the core, that is, the connections between high-degree core nodes has a significant impact on the distribution. Thus, the above-mentioned three principles marked as **P1**, **P2**, and **P3** are helpful in preserving the distribution.

4 Random node sampling for evaluating parameters

Core-periphery detection^[26] refers to a partition of a network into two groups of nodes called core and periphery, which is a useful tool to realize P1. An important procedure of the detection is to provide rank orders of nodes for the partition. Many measures based on clique, community, centrality, and probability^[12-15,26], have been adopted for the rank. These complex measures can help improve detection accuracy, but are difficult to be quickly evaluated on unknown networks. Thus, we use a simple measure, namely degree, to rank the nodes, and design a random node sampling to evaluate the AD and DT of the unknown networks that are critical for P1 and P3. Specifically, nodes with degrees larger than DT are classified to the core, while other nodes are divided to the periphery. To clearly distinguish the core nodes and periphery nodes, the DT is determined by maximizing the number of edges connecting the two types of nodes.

Please note that our random node sampling is different from the RN sampling^[5] introduced in Section 2.1 that generates a subgraph induced by randomly chosen nodes. Our sampling collects the degrees $d_{org}(v)$ and neighbors $N_{org}(v)$ of the randomly chosen nodes in the unknown networks, and evaluates the AD and DT of the unknown networks based on the degrees and neighbors.

The random node sampling has a shortcoming in the capture of high-degree nodes, since nodes with higher degrees correspond to a lower percentage in the original scale-free network. However, owing to the low percentage of the nodes, the loss of their high degrees has almost no impact on the AD evaluation. Please note that the evaluated AD is much larger than the AD of the subgraph generated by the RN sampling^[5], because many important high-degree nodes are lost in the subgraph, but not lost in our collected neighbor set $N_{org}(v)$ that is defined as the set of the neighbor nodes of v in the unknown graph G_{org} , not in the RN sampled subgraph^[5] (seeing Section 6.3.5).

Random node sampling: Evaluating the AD and DT

- 1: **Input:** A sampling rate R , and an original network $G_{org} = (V_{org}, E_{org})$ with unknown topological information, but the node set and the neighbors of sampled nodes in the network can be accessed.
- 2: **Output:** \bar{d}_{org} , namely the evaluated AD, and \ddot{d}_{org} , namely the evaluated DT, of G_{org} .
- 3: Randomly extract $\|V_{org}\| \times R$ nodes from V_{org} with uniform distribution to form a node set V , and derive $d_{max} = \max\{d_{org}(v) | v \in V\}$.
- 4: Initialize $vertical_edge_set \leftarrow \emptyset$ that consists of vertical edges defined as the edges connected by a periphery node and a core node.
We assume v is a periphery node and u is a core node for each edge $(v, u) \in vertical_edge_set$.
- 5: Initialize $k \leftarrow 1$, and $\ddot{d}_{org} \leftarrow 0$.
- 6: **While** $k \leq d_{max}$ **do**
- 7: Update $\ddot{d}_{org} \leftarrow k$, and derive a node set $V_k = \{v | v \in V \wedge d_{org}(v) = \ddot{d}_{org}\}$.
- 8: Derive two sets caused by the update of \ddot{d}_{org} from $k-1$ to k , namely, $added_edge_set$, which consists of edges that are newly added to $vertical_edge_set$, and $removed_edge_set$, which consists of edges that should be removed from $vertical_edge_set$.

$$added_edge_set = \{(v, u) | v \in V_k \wedge u \in N_{org}(v) \wedge d_{org}(u) > \ddot{d}_{org}\}$$

$$removed_edge_set = \{(v, u) | (v, u) \in vertical_edge_set \wedge d_{org}(v) < \ddot{d}_{org} \wedge d_{org}(u) = \ddot{d}_{org}\}$$
 Update $vertical_edge_set \leftarrow vertical_edge_set \cup added_edge_set - removed_edge_set$.
- 9: **If** $\|added_edge_set\| \leq \|removed_edge_set\|$ **do** Update $\ddot{d}_{org} \leftarrow k-1$; **Break;** **End If**
- 10: Update $k \leftarrow k+1$.
- 11: **End While** %Please note that $N_{org}(v)$ is the set of neighbor nodes of node v in G_{org} , not in the subgraph induced by the node set V .
- 12: Derive $\bar{d}_{org} \leftarrow \sum_{v \in V} d_{org}(v) / \|V\|$, and output \bar{d}_{org} and \ddot{d}_{org} . %Please note that $d_{org}(v) = \|N_{org}(v)\|$.

Let us return to the pseudocode of our random node sampling. Assuming that \ddot{d}_{org} in line 7 is not more than the actual DT value, then the V_k nodes and the nodes u with $d_{org}(u) = \ddot{d}_{org}$ in $removed_edge_set$ (in line 8) are classified into the periphery, that is,

$$\|added_edge_set\| > \|removed_edge_set\|, \quad (1)$$

because $added_edge_set$ (in line 8) contains the edges that connect the peripheral V_k nodes to core nodes in the original network G_{org} , and $removed_edge_set$ consists of the edges connecting two periphery nodes. Please note that there are dense connections between core and periphery nodes but sparse connections between periphery nodes^[12-15,26]. Although the set V in line 3 losses top highest degree nodes in the core, most of nodes in V can quickly reach the core through only one jump, since the PA rule^[25] causes the core to be densely connected by the periphery^[12-15,26], which ensures that the information of the top highest degree nodes is not lost in $added_edge_set$. In addition, owing to the weak correlation (i.e., sparse connections) between each other, the periphery nodes in V obtained by a low sampling rate are sufficient to accurately evaluate the DT value.

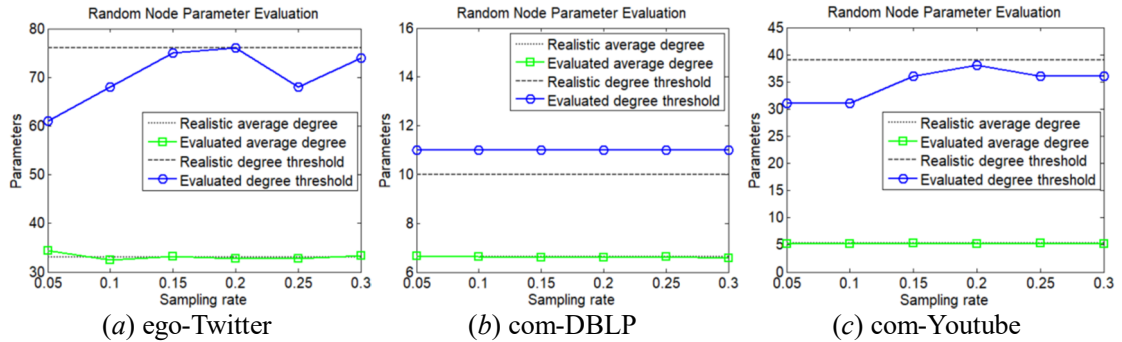


Fig. 1. The evaluated AD and DT vs. sampling rate R on three original networks extracted from Stanford Large Network Dataset Collection^[27]. Please note that the realistic values of AD and DT are related to $R = 100\%$, and the three original networks are illustrated in Section 6.

The experimental results on \bar{d}_{org} vs. R and \ddot{d}_{org} vs. R are shown in Fig. 1, which tell us that a low sampling rate R set to 15% by default is competent for the evaluation. Using the evaluated degree threshold \ddot{d}_{org} , five commonly-used and scale-free original networks^[27], which are

illustrated in Section 6 for evaluation, are partitioned into core-periphery structures, as shown in Table 2, in which all edges in the original networks are classified into core edges that connect two core nodes, vertical edges that connect a core node and a periphery node, and periphery edges that connect two periphery nodes. The percentage distributions of nodes and edges in Table 2 confirm to the structure of dense core and sparse periphery [12-15,26].

Table 2. Percentage distributions of nodes and edges in the core-periphery structures

Original networks [27]	\ddot{d}_{org}	Node percentage distribution		Edge percentage distribution		
		Core	Periphery	Core	Vertical edges	Periphery
ego-Twitter	75	10%	90%	26%	47%	27%
loc-Gowalla	32	5%	95%	26%	39%	35%
com-DBLP	11	13%	87%	28%	42%	30%
web-Stanford	38	4%	96%	15%	58%	27%
com-Youtube	36	2%	98%	17%	51%	32%

Further analysis of the random node sampling can be seen in Section 6.3.5.

5 Unknown network sampling SLSR

Our SLSR creates a core-periphery framework for existing traversal-based samplings, such as RWR [5], FF [17], CNARW [18] and RD [19]. First, choose one sampling from the existing methods and use T_s to represent it, then SLSR restricts T_s to only traverse on the periphery using the evaluated \ddot{d}_{org} . Specifically, the set of neighbors of a node v that is accessing by T_s is changed as

$$N_{org}^{per}(v) = \{u | u \in N_{org}(v) \wedge d_{org}(u) \leq \ddot{d}_{org}\} \quad (2)$$

and other principles and steps of T_s remain unchanged. Please note that, the other neighbor set

$$N_{org}^{cor}(v) = \{u | u \in N_{org}(v) \wedge d_{org}(u) > \ddot{d}_{org}\} \quad (3)$$

that is obtained simultaneously with Eq. (2) should be saved for the core sampling. The process of T_s running on the periphery of G_{org} with a sampling rate R is represented as follows:

$$G_{sub}^{per} = (V_{sub}^{per}, E_{sub}^{per}), \{N_{org}^{cor}(v) | v \in V_{sub}^{per}\} \leftarrow PeripherySampling(T_s, G_{org}, \ddot{d}_{org}, R) \quad (4)$$

where G_{sub}^{per} denotes the sampled subgraph of the periphery, and V_{sub}^{per} and E_{sub}^{per} denote its node set and edge set. According to P3, predefine a parameter $x\%$ to preserve top- $(\|N_{org}^{cor}(v)\| \times x\%)$ highest degree core neighbors for each $v \in V_{sub}^{per}$, and let V_{sub}^{cor} denote the set composed of all the preserved core neighbors. Please note that, the vertical edge set

$$E_{sub}^{ver} = \{(v, u) | v \in V_{sub}^{per} \wedge u \in N_{org}^{cor}(v) \cap V_{sub}^{cor}\} \quad (5)$$

should be preserved. According to P2, all the connections between V_{sub}^{cor} nodes in G_{org} also should be preserved, which can be implemented by the access of the neighbors of each V_{sub}^{cor} node in G_{org} . Please note that the V_{sub}^{cor} nodes and the connections between them construct the sampled core.

Next, analyze how to determine the parameter $x\%$. With the growth of $x\%$, the number of the vertical edges (namely, $\|E_{sub}^{ver}\|$) increases, while the sampled periphery G_{sub}^{per} remains unchanged and the sampled core induced by the node set V_{sub}^{cor} has a low variability [15]. Thus, the AD of the subgraph, composed of the vertical edges and the sampled periphery and sampled core, increases monotonically as $x\%$ grows, that is, a bisection method can be used to determine $x\%$ under the guidance of the evaluated \ddot{d}_{org} that is our target AD of the sampled subgraph.

Bisection method: Determining the parameter $x\%$

- 1: **Input:** The sampled periphery $G_{sub}^{per} = (V_{sub}^{per}, E_{sub}^{per})$, the core neighbor sets $\{N_{org}^{cor}(v) | v \in V_{sub}^{per}\}$, the original network $G_{org} = (V_{org}, E_{org})$, and \bar{d}_{org} that is the evaluated AD of G_{org} .
 - 2: **Output:** $x\%$.
 - 3: Initialize $x_{min} \leftarrow 1$, $x_{max} \leftarrow 100$, and $min_distance \leftarrow 1000$.
 - 4: **While** $x_{max} - x_{min} > 1$ **do**
 - 5: Update $x \leftarrow [(x_{max} + x_{min})/2]$, and $x\% \leftarrow x/100$, where $[X]$ rounds the element X to the nearest integer.
 - 6: Initialize $V_{sub}^{cor} \leftarrow \emptyset$ and $E_{sub}^{per} \leftarrow \emptyset$.
 - 7: **For each** node $v \in V_{sub}^{per}$, assume $N_{org}^{cor}(v) = \{u_1, u_2, \dots, u_t\}$ with $d_{org}(u_1) \geq d_{org}(u_2) \geq \dots \geq d_{org}(u_t)$, where $t = \|N_{org}^{cor}(v)\|$.
 - 8: Derive $k \leftarrow \lceil \|N_{org}^{cor}(v)\| \times x\% \rceil$, and update $V_{sub}^{cor} \leftarrow V_{sub}^{cor} \cup \{u_1, u_2, \dots, u_k\}$ and $E_{sub}^{per} \leftarrow E_{sub}^{per} \cup \{(v, u_1), (v, u_2), \dots, (v, u_k)\}$.
 - 9: **End For**
 - 10: Derive a sampled core $G_{sub}^{cor} = (V_{sub}^{cor}, E_{sub}^{cor})$ that preserves all the connections between V_{sub}^{cor} nodes in G_{org} , and a sampled subgraph $G_{sub} = (V_{sub}, E_{sub})$ where $V_{sub} = V_{sub}^{cor} \cup V_{sub}^{per}$ and $E_{sub} = E_{sub}^{cor} \cup E_{sub}^{per} \cup E_{sub}^{per}$.
 - 11: Derive the average degree $\bar{d}_{sub} = 2\|E_{sub}\|/\|V_{sub}\|$ of G_{sub} .
 - 12: **If** $\bar{d}_{sub} \geq \bar{d}_{org}$, **then** update $x_{max} \leftarrow x$, **Else** update $x_{min} \leftarrow x$. **End If**
 - 13: **If** $|\bar{d}_{sub} - \bar{d}_{org}| < min_distance$, **then** update $x_{opt} \leftarrow x$ and $min_distance \leftarrow |\bar{d}_{sub} - \bar{d}_{org}|$. **End If**
 - 14: **End While**
 - 15: Output $x\%$ where $x = x_{opt}$.
-

Please note that the number of iterations of the While loop in the bisection method is not more than $\log_2 100$. Moreover, $\|N_{org}^{cor}(v)\| < \bar{d}_{org}$ for each $v \in V_{sub}^{per}$ in line 7, and $\|V_{sub}^{cor}\| \ll \|V_{sub}^{per}\|$ in line 10, since the scale of the core is much smaller than that of the periphery, as shown in Table 2. Thus, the time complexity of the bisection method is $O(\|V_{sub}^{per}\|)$. Once the parameter $x\%$ is determined, the sampled subgraph of G_{org} can be obtained using lines 6 to 10 in the bisection method. The Main function of SLSR is described as follows:

SLSR: Main function

- 1: **Input:** A sampling rate R , and an original network $G_{org} = (V_{org}, E_{org})$ with unknown topological information but the node set and the neighbors of sampled nodes in the network can be accessed; \bar{d}_{org} , namely the evaluated AD, and \bar{d}_{org} , namely the evaluated DT, of G_{org} .
 - 2: **Output:** $G_{sub} = (V_{sub}, E_{sub})$, namely a sampled subgraph of G_{org} , where V_{sub} and E_{sub} respectively denote the sampled node set and edge set.
 - 3: Choose an existing traversal-based sampling T_s , and run T_s on the periphery of G_{org} based on \bar{d}_{org} :

$$G_{sub}^{per} = (V_{sub}^{per}, E_{sub}^{per}), \{N_{org}^{cor}(v) | v \in V_{sub}^{per}\} \leftarrow \text{PeripherySampling}(T_s, G_{org}, \bar{d}_{org}, R).$$
 - 4: Determine the parameter $x\%$ using the above-mentioned bisection method.
 - 5: Obtain $G_{sub} = (V_{sub}, E_{sub})$ under the constraint of $x\%$, and output the sampled subgraph.
- Please note that the obtainment process is the same as lines 6 to 10 in the above-mentioned bisection method.
-

The sampling framework created by SLSR is simple. Simpler methods typically have higher time efficiency. However, the framework can significantly improve the accuracy of multi-structure preservation for T_s at low sampling rates.

PeripherySampling: Choosing T_s as the FF sampling^[17]

- 1: **Input:** $G_{org} = (V_{org}, E_{org})$, \bar{d}_{org} , and R .
 - 2: **Output:** $G_{sub}^{per} = (V_{sub}^{per}, E_{sub}^{per})$, and $\{N_{org}^{cor}(v) | v \in V_{sub}^{per}\}$.
 - 3: Create an empty FIFO (first-in-first-out) queue Q where $Q \leftarrow v$ represents adding v to Q and $v \leftarrow Q$ represents extracting and deleting v from Q .
 - 4: Derive $n = \|V_{org}\| \times R$ that represents the expected number of nodes to be sampled, and initialize $V_{sub}^{per} \leftarrow \emptyset$ and $E_{sub}^{per} \leftarrow \emptyset$.
 - 5: Randomly choose a seed w that falls in $\{v | v \in V_{org} \wedge d_{org}(v) \leq \bar{d}_{org}\} - V_{sub}^{per}$, and $Q \leftarrow w$.
 - 6: **While** $\|V_{sub}^{per}\| < n$ **do**:
 - 7: **If** Q is empty, **then** randomly choose a seed w that falls in $\{v | v \in V_{org} \wedge d_{org}(v) \leq \bar{d}_{org}\} - V_{sub}^{per}$, and $Q \leftarrow w$. **End If**
 - 8: $v \leftarrow Q$; Derive $N_{org}^{cor}(v) = \{u | u \in N_{org}(v) \wedge d_{org}(u) > \bar{d}_{org}\}$ and $N_{org}^{per}(v) = \{u | u \in N_{org}(v) \wedge d_{org}(u) \leq \bar{d}_{org}\}$.
 - 9: Update $E_{sub}^{per} \leftarrow E_{sub}^{per} \cup \{(v, u) | u \in N_{org}^{per}(v) \cap V_{sub}^{per}\}$, and update $V_{sub}^{per} \leftarrow V_{sub}^{per} \cup \{v\}$.
 - 10: **If** $\|V_{sub}^{per}\| + \|Q\| < n$, **then** extract a fraction of nodes in $N_{org}^{per}(v) - V_{sub}^{per} - Q$, where the fraction is randomly drawn from a geometric distribution, and add the nodes into Q . **End If**
 - 11: **End While** %The probability of that w in lines 5 and 7 falls into the periphery $\{v | v \in V_{org} \wedge d_{org}(v) \leq \bar{d}_{org}\}$ is very high based on Table 2.
 - 12: Output $G_{sub}^{per} = (V_{sub}^{per}, E_{sub}^{per})$ and $\{N_{org}^{cor}(v) | v \in V_{sub}^{per}\}$.
-

For comparative verification, we arbitrarily choose T_s as the FF sampling^[17], since the sampling traverses each node no more than once which leads to its high time efficiency. Please note that users can use T_s to represent other existing traversal-based samplings. Once T_s is chosen, the periphery sampling can be determined.

6 Evaluation

6.1 Metrics

AD is defined as $\sum kP(k) = 2\|E\|/\|V\|$ in a simple and undirected graph $G = (V, E)$ with node set V and edge set E , where $P(k)$ denotes the fraction of nodes with degree k in G ^[28-30]. The statistic reflects whether a sampling favors core nodes with high-degrees.

Complementary cumulative distribution defined as $F(k)$ vs. k where $F(k) = \sum_{d>k} P(d)$ exhibits better degree power-law characteristic^[28]

Average clustering coefficient (ACC) defined as $\bar{C} = \sum C(k)P(k)$ represents how close a node's neighbors are to forming a clique^[31-33], where $C(k) = 2T(k)/k(k-1)$ and $T(k)$ denotes the average of the number of links between two neighbors of k -degree nodes. A related distribution characteristic is **clustering coefficient distribution**^[31] defined as $C(k)$ vs. k .

Average path length (APL) is defined as $\bar{L} = \sum l \cdot \mu(l)$ that represents the reachability of nodes within each other, where $\mu(l)$ denotes the fraction of node pairs with shortest path length l between the two nodes. A related distribution characteristic is shortest **path length distribution** that is defined as $\mu(l)$ vs. l ^[31,33].

Assortativity coefficient (AC) is defined as^[34-36]

$$r = \frac{\sum_i j_i k_i - M^{-1} \sum_i j_i \sum_i k_i}{\sqrt{[\sum_i j_i^2 - M^{-1} (\sum_i j_i)^2][\sum_i k_i^2 - M^{-1} (\sum_i k_i)^2]}} \quad (6)$$

where j_i and k_i denote the degrees of the two nodes connected by the i^{th} edge, and $M = \|E\|$. AC represents whether nodes with similar degrees tend to connect with each other^[34-36], which is a critical statistic to reflect a sampling's preference for high-degree core nodes.

Ratio of weighted spectral distribution to node number (RWSD) represents the connection relationship between low-degree nodes^[37] most of which are in the periphery. The weighted spectral distribution is defined as $\sum (1 - \lambda_i)^4$ where λ_i denotes the i^{th} eigenvalue in the normalized Laplacian spectrum of G ^[37-39]. Please note that the statistic can be quickly calculated by a 4-cycle enumeration algorithm without the need for the calculation of the eigenvalues^[40].

Ratio of maximum degree to node number (RMD) represents the influence of the node with maximum degree, which is suitable for the comparison of graphs with different scales^[41].

Closeness centrality (CC) of a node is defined as $(n-1)/L$ where n is the total number of nodes and L denotes the sum of the length of the shortest path from the node to other nodes, which reflects how efficiently the node exchanges information with others^[42].

Betweenness centrality (BC) of a node represents the fraction of the shortest paths that pass through the node for any pair of nodes, which describes potential power of the node in controlling the information flow in a network^[43,44].

Community represents local densely-connected structures that are visually salient^[45,46]. Thus, a visual evaluation was adopted. Specifically, the communities were detected by a Louvain method^[46] and visually displayed by a force-directed method^[47]. Meanwhile, the correspondence between the communities of an original network and sampled graphs was established by their shared nodes.

6.2 Original networks

The above multiple metrics and five widely-used large original networks chosen from Stanford Large Network Dataset Collection ^[27] are adopted for the evaluation. Please note that the original networks listed in Table 3 are simplified as undirected graphs, and the self-loops, multi-edges, and direction of edges in the networks are removed. In addition, the important statistics of the original networks have been listed in Tables 4 to 8 for the convenience of comparison.

Table 3. Descriptions of the five widely-used large original networks ^[27]

Original networks	Node number	Edge number	Descriptions
ego-Twitter	81,306	1,768,149	This dataset consists of 'circles' (or 'lists') from Twitter.
loc-Gowalla	196,591	950,327	This dataset consists of a location-based social network where users share their locations by checking-in.
com-DBLP	317,080	1,049,866	This dataset consists of a co-authorship network from DBLP that is a computer science bibliography.
web-Stanford	281,903	2,312,497	This dataset consists of a web network from Stanford University (stanford.edu).
com-Youtube	1,134,890	2,987,624	This dataset consists of a social network from Youtube that is a video-sharing web site.

6.3 Comparisons

Our SLSR is compared with the related traversal-based samplings, namely FF ^[17], CNARW ^[18], RWR ^[5] and RD ^[19], on the five large original networks introduced in Table 3.

6.3.1 Statistics

Restricted by low sampling rates, the traditional traversal-based samplings have an excessive preference for densely-connected core nodes, while SLSR can effectively solve this problem using a two-layer sampling strategy. Specifically, the five statistics introduced in Section 6.1, namely AD, APL, AC, RWSD and RMD, were chosen to measure the excessive preference.

A high degree node is connected by a large number of edges, that is, AD becomes larger as the preference is stronger. Periphery nodes shorten the path length between each other through the core, that is, APL becomes smaller as the preference is stronger. According to the study of Jiao et al. ^[37], the RWSD strictly indicates the feature of connections between low-degree nodes on large networks, and the statistic becomes smaller as the connections become sparser. Please note that the low-degree nodes are mainly located in the periphery and the excessive preference induces sparser connections between the periphery nodes (i.e., smaller RWSD).

Table 4. Comparison of statistics between the original ego-Twitter network and its subgraphs sampled by SLSR and related methods with sampling rate $R = 5\%$, where v_{org}^{max} is the maximum degree node in the original network, and the node is preserved in the sampled subgraphs.

Statistics		AD	ACC	APL	AC	RWSD	RMD	$CC(v_{org}^{max})$	$BC(v_{org}^{max})$
Original network		33.01	0.565	3.889	-0.039	0.008	0.042	0.402	0.059
Sampled subgraphs with $R = 5\%$	SLSR	32.93	0.482	3.247	-0.022	0.009	0.176	0.407	0.022
	FF	59.16	0.535	2.590	-0.133	0.005	0.595	0.441	0.017
	CNARW	31.94	0.454	3.296	+0.047	0.014	0.143	0.446	0.047
	RWR	55.06	0.533	2.780	-0.142	0.011	0.566	0.448	0.029
	RD	6.845	0.005	5.367	-0.119	0.085	0.063	0.295	0.128

Table 5. Comparison of statistics between the original loc-Gowalla network and its subgraphs sampled by SLSR and related methods with sampling rate $R = 5\%$, where v_{org}^{max} is the maximum degree node in the original network, and the node is preserved in the sampled subgraphs.

Statistics		AD	ACC	APL	AC	RWSD	RMD	$CC(v_{org}^{max})$	$BC(v_{org}^{max})$
Original network		9.66	0.236	4.627	-0.029	0.057	0.075	0.389	0.324
Sampled subgraphs with $R = 5\%$	SLSR	9.79	0.228	4.512	-0.029	0.080	0.135	0.404	0.390
	FF	26.98	0.289	3.250	-0.065	0.017	0.251	0.524	0.257
	CNARW	22.13	0.261	3.599	-0.058	0.036	0.217	0.483	0.274
	RWR	26.49	0.292	3.236	-0.078	0.024	0.260	0.526	0.252
	RD	5.778	0.142	3.672	-0.159	0.103	0.262	0.481	0.454

Table 6. Comparison of statistics between the original com-DBLP network and its subgraphs sampled by SLSR and related methods with sampling rate $R = 10\%$, where v_{org}^{max} is the maximum degree node in the original network, and the node is preserved in the sampled subgraphs.

Statistics		AD	ACC	APL	AC	RWSD	RMD	$CC(v_{org}^{max})$	$BC(v_{org}^{max})$
Original network		6.621	0.632	6.792	0.266	0.070	0.001	0.218	0.007
Sampled subgraphs with $R = 10\%$	SLSR	6.183	0.552	6.805	0.322	0.099	0.002	0.217	0.012
	FF	10.08	0.541	5.432	0.641	0.048	0.007	0.258	0.010
	CNARW	7.535	0.448	6.031	0.361	0.068	0.004	0.238	0.010
	RWR	9.456	0.525	5.297	0.509	0.056	0.006	0.259	0.008
	RD	6.985	0.239	5.809	0.158	0.065	0.006	0.245	0.012

Table 7. Comparison of statistics between the original web-Stanford network and its subgraphs sampled by SLSR and related methods with sampling rate $R = 10\%$, where v_{org}^{max} is the maximum degree node in the original network, and the node is preserved in the sampled subgraphs.

Statistics		AD	ACC	APL	AC	RWSD	RMD	$CC(v_{org}^{max})$	$BC(v_{org}^{max})$
Original network		14.14	0.597	6.815	-0.112	0.049	0.137	0.279	0.632
Sampled subgraphs with $R = 10\%$	SLSR	14.12	0.564	5.157	-0.144	0.037	0.171	0.359	0.663
	FF	33.91	0.631	4.333	-0.148	0.018	0.261	0.390	0.505
	CNARW	28.13	0.593	4.447	-0.226	0.018	0.323	0.412	0.651
	RWR	30.00	0.626	2.222	-0.307	0.011	0.872	0.862	0.476
	RD	5.321	0.315	4.701	-0.247	0.058	0.165	0.385	0.688

Table 8. Comparison of statistics between the original com-YouTube network and its subgraphs sampled by SLSR and related methods with sampling rate $R = 5\%$, where v_{org}^{max} is the maximum degree node in the original network, and the node is preserved in the sampled subgraphs.

Statistics		AD	ACC	APL	AC	RWSD	RMD	$CC(v_{org}^{max})$	$BC(v_{org}^{max})$
Original network		5.265	0.081	5.279	-0.036	0.081	0.025	0.338	—
Sampled subgraphs with $R = 5\%$	SLSR	5.132	0.096	5.919	-0.018	0.134	0.056	0.316	—
	FF	23.03	0.131	3.918	-0.033	0.025	0.119	0.446	—
	CNARW	19.73	0.110	4.051	-0.046	0.038	0.120	0.432	—
	RWR	19.36	0.156	3.685	-0.123	0.022	0.119	0.445	—
	RD	5.480	0.062	4.444	-0.099	0.101	0.088	0.383	—

AC ranges from -1 to 1 . Specifically, AC falling in $(0,1]$ defines an assortativity network, where high degree nodes tend to connect other high degree nodes, whereas AC falling in $[-1,0)$ defines a disassortativity network, where high degree nodes tend to connect lower-degree nodes^[34]. In addition, AC quantifies whether nodes with similar degrees tend to connect with each other^[34-36]. Thus, AC in the assortativity network strongly depends on the connections between core nodes that have similar high degrees, and the excessive preference for core nodes induces larger AC; whereas, AC in the disassortativity network is mainly determined by the connections between periphery nodes that have similar low degrees, and the excessive preference for core nodes, which leads to sparser connections between the periphery nodes, induces smaller AC in general.

In addition, the excessive preference for core nodes generally induces larger RMD because the maximum degree node must be located in the core.

Please note that we chose T_s in SLSR as the FF sampling for the experiments. Thus, we first compare the results between SLSR and FF. Based on the above-mentioned analysis associated with the five statistics and their performance in Tables 4 to 8, FF has an excessive preference for the core, whereas SLSR solves the issue. A recent sampling CNARW also solves the issue in Tables 4 and 6. We return to Table 2 which shows that the core node percentages in the ego-Twitter and com-DBLP networks are obviously larger than those in other networks, that is, the core in the two networks is larger and sparser, which is critical for the well performance of CNARW in Tables 4 and 6. The RD sampling starts with a certain number of randomly chosen seed nodes and the number is predetermined as $0.01 \times \|V_{org}\|$ by default, which is helpful in avoiding the sampling trapped locally in the periphery^[19]. However, the strategy of multiple initial seeds is prone to loss of core nodes at low sampling rates, which disrupts the connectivity of the original networks.

According to the analysis in Section 3, P1, P2 and P3 adopted by SLSR are helpful in capturing ACC, which can be verified by Tables 4 to 8.

In addition, we compare two centralities (i.e., CC and BC) of some important nodes between the original networks and their sampled subgraphs. The nodes were chosen as the maximum degree nodes v_{org}^{max} in the original networks, and they can be preserved to the sampled subgraphs by the biased samplings being compared. The chosen T_s in SLSR is competent for capturing peripheral degree distribution without the interference of the core, all the edges that connect v_{org}^{max} to nodes in V_{sub}^{per} are preserved due to P3, where $G_{sub}^{per} = (V_{sub}^{per}, E_{sub}^{per})$ is the output of T_s , and the structure of the core is preserved to the maximum extent possible due to P2. All the clues strongly influence the centralities of the top highest degree core nodes in the SLSR sampled subgraphs, and Tables 4 to 8 verify that the clues are helpful in capturing $CC(v_{org}^{max})$ and $BC(v_{org}^{max})$.

$BC(v_{org}^{max})$ of the original com-Youtube network with 1,134,890 nodes and 2,987,624 edges was not provided in Table 8 due to extremely high computation and memory requirements. Please note that the RWSD of the network can be quickly obtained within 2 hours^[40], whereas the APL and the path length distribution of the network have to be computed by a parallel algorithm. On a computer with Intel Core i7-8700 CPU 3.20 GHz Memory 16 G, the parallel algorithm with 5 threads used for calculating the APL and the path length distribution runs about 12 days.

According to the above analysis, SLSR has the best comprehensive performance on the eight chosen statistics, since it performs well on both types of original networks, one with relatively large and sparse cores, such as Tables 4 and 6, and the other with relatively small and dense cores, such as Tables 5, 7 and 8. Please note that Table 2 shows the core information.

6.3.2 Distributions

The distribution comparisons are shown in Figs. 2 to 6.

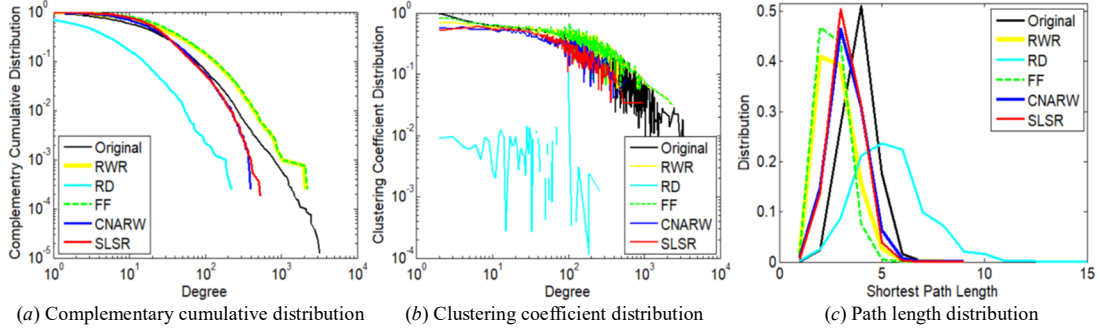


Fig. 2. Comparison of distribution characteristics between original ego-Twitter network and its subgraphs sampled by SLSR and related methods with sampling rate $R = 5\%$.

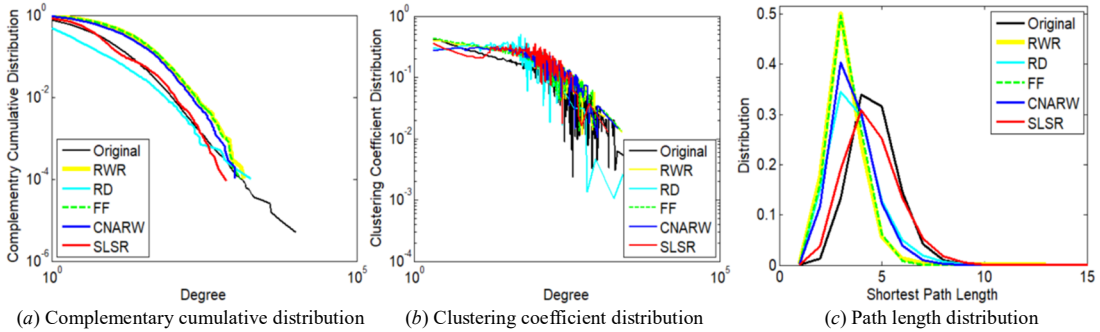


Fig. 3. Comparison of distribution characteristics between original loc-Gowalla network and its subgraphs sampled by SLSR and related methods with sampling rate $R = 5\%$.

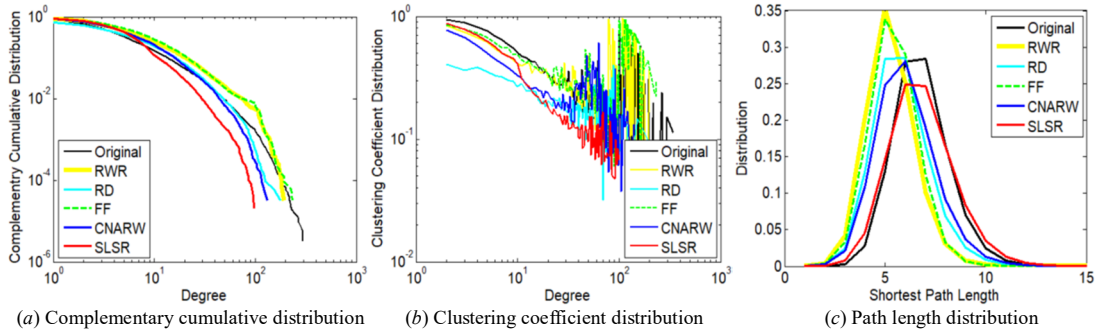


Fig. 4. Comparison of distribution characteristics between original com-DBLP network and its subgraphs sampled by SLSR and related methods with sampling rate $R = 10\%$.

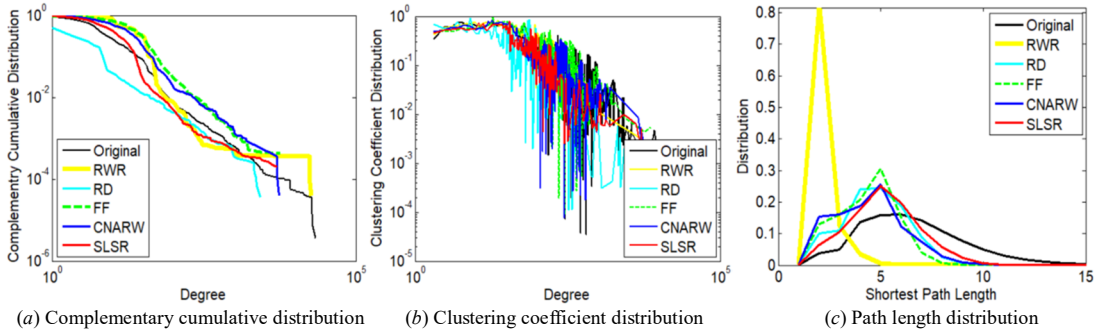


Fig. 5. Comparison of distribution characteristics between original web-Stanford network and its subgraphs sampled by SLSR and related methods with sampling rate $R = 10\%$.

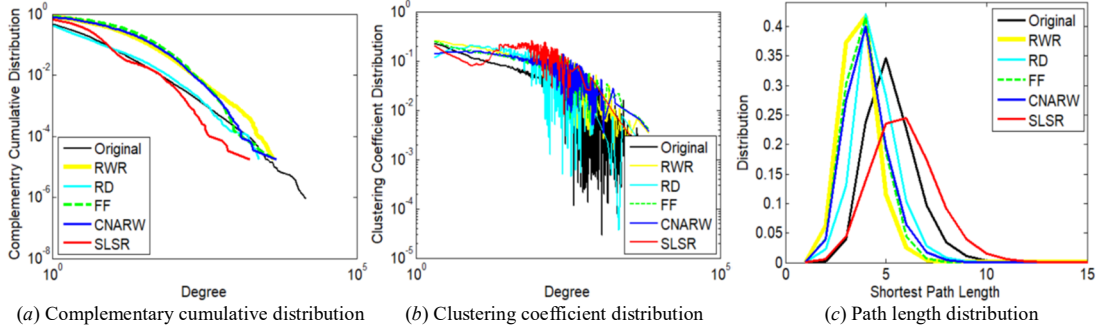


Fig. 6. Comparison of distribution characteristics between original com-YouTube network and its subgraphs sampled by SLSR and related methods with sampling rate $R = 5\%$.

Degree complementary cumulative distribution [28], clustering coefficient distribution [31], and path length distribution [31,33], which are commonly-used measures, are chosen for the comparison. Please note that, the distribution with lower degrees is more important for the first two measures. For example, in Fig. 4(a) and (b), degrees not exceeding 20 correspond to 95% of the total number of nodes in the com-DBLP network. Based on the comparisons of Figs. 2 to 6, SLSR has the best comprehensive performance on the three distributions.

6.3.3 Community visualization

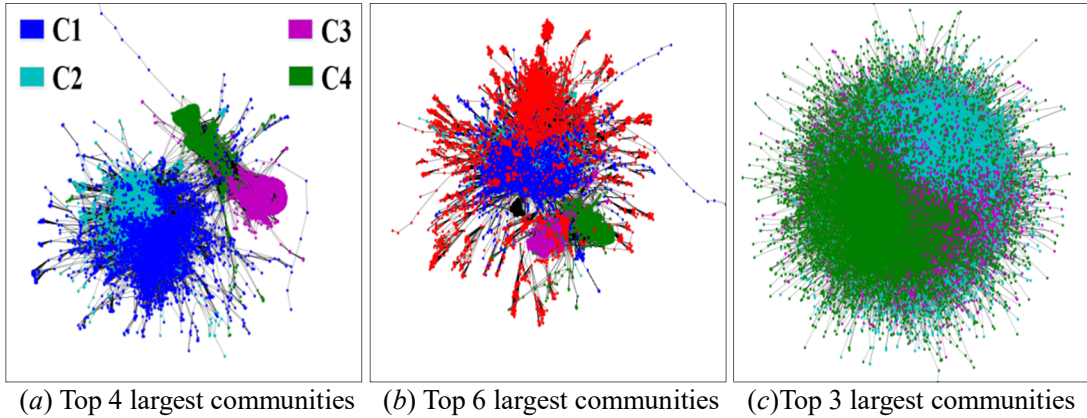


Fig. 7. Visualization of top largest communities in the (a)(b) original web-Stanford network and the (c) original loc-Gowalla network. Specifically, the top 4 largest communities in (a) are named as C1, C2, C3 and C4, respectively.

Force-directed layout [47] is a powerful visualization tool for communities, but has two shortcomings when applied to large networks. One is that communities overlap severely with each other, the other is that the layout speed is extremely slow. To make up for the shortcomings, we first use a Louvain method [46] to detect the communities of an original network and its sampled subgraphs, and then extract top- k largest communities and visualize them. As shown in Fig.7, the boundaries of distinct communities in the original web-Stanford network are clearer than those in the original loc-Gowalla network. Thus, we chose the former for the visualization comparison.

Let $C_i = (V_{ci}, E_{ci})$ denote a community in Fig. 7(a), and $S = (V_s, E_s)$ denote a community in Figs. 8(a) to 12(a). If $r_s = \|V_s \cap V_{ci}\|/\|V_s\| \geq 25\%$, we believe that S in the sampled subgraphs originates from C_i in the original network. Please note that all information about $r_s \geq 25\%$ has been marked in Figs. 8(a) to 12(a). Fig. 7(a)(b) shows that C_1 and C_2 gather with other communities and the boundaries between them are vague, while C_3 and C_4 are remote communities far from the gathering center. Figs. 8(a) to 12(a) show that only SLSR and RD can capture C_3 and C_4 , while

other samplings lost them. RD avoids getting stuck locally by a large number of initial random seeds, but causes subgraphs to be decomposed into many disconnected components. SLSR allows T_s to traverse more remote communities in the periphery by peeling off the core, while maintaining the connectivity of the sampled subgraphs using P2 and P3.

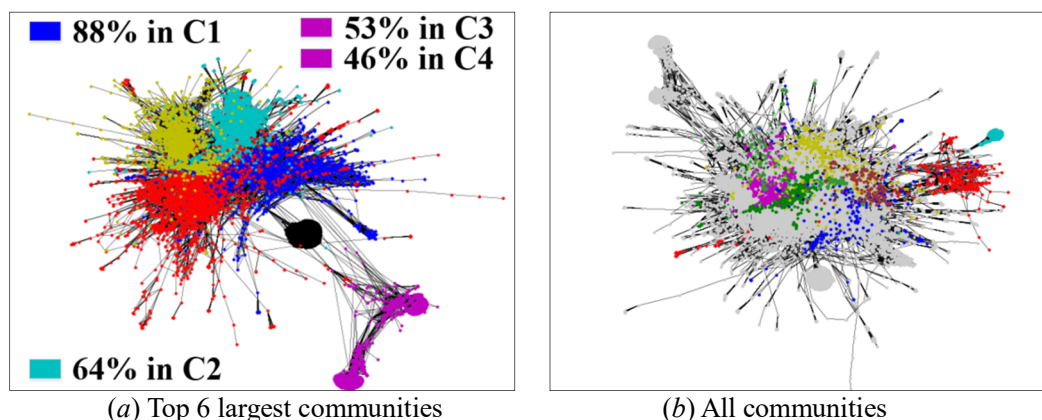


Fig. 8. Visualization of communities in a sampled subgraph of the web-Stanford network, where the subgraph was obtained by SLSR with $R = 10\%$. (a) Top 6 largest communities, in which 88% of blue nodes are in C1, 64% of cyan nodes are in C2, 53% of magenta nodes are in C3, and 46% of magenta nodes are in C4. (b) All communities, in which top 10 largest communities are marked as white, and other small communities are marked in color.

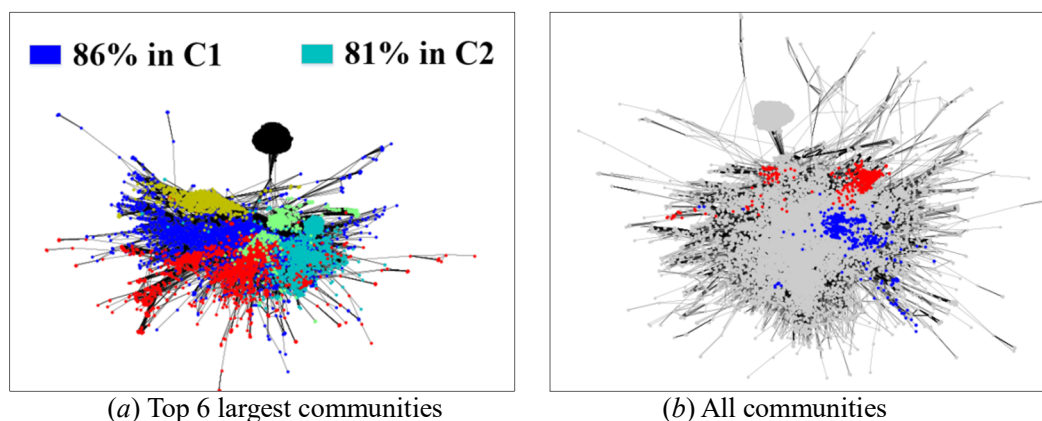


Fig. 9. Visualization of communities in a sampled subgraph of the web-Stanford network, where the subgraph was obtained by FF with $R = 10\%$. (a) Top 6 largest communities, in which 86% of blue nodes are in C1, 81% of cyan nodes are in C2. **Please note that C3 and C4 are lost.** (b) All communities, in which top 10 largest communities are marked as white, and other small communities are marked in color.

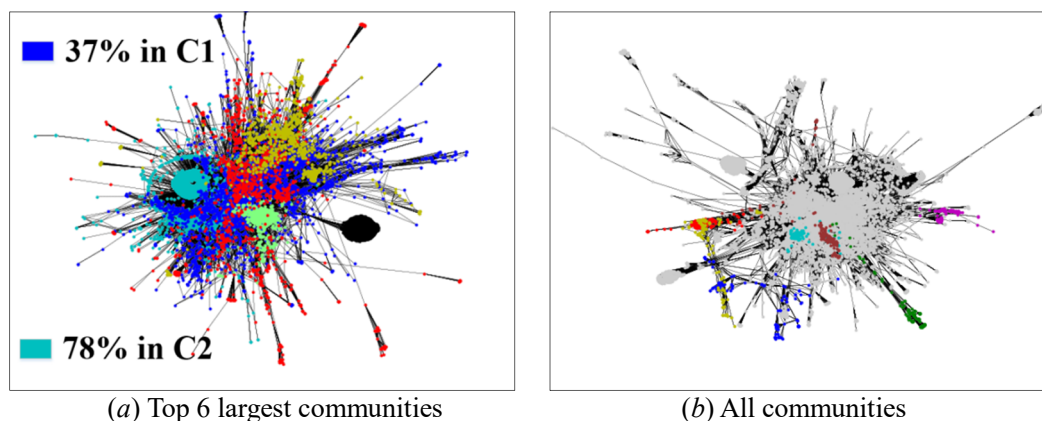


Fig. 10. Visualization of communities in a sampled subgraph of the web-Stanford network, where the subgraph was obtained by **CNARW** with $R = 10\%$. (a) Top 6 largest communities, in which 37% of blue nodes are in C1, 78% of cyan nodes are in C2. **Please note that C3 and C4 are lost.** (b) All communities, in which top 10 largest communities are marked as white, and other small communities are marked in color.

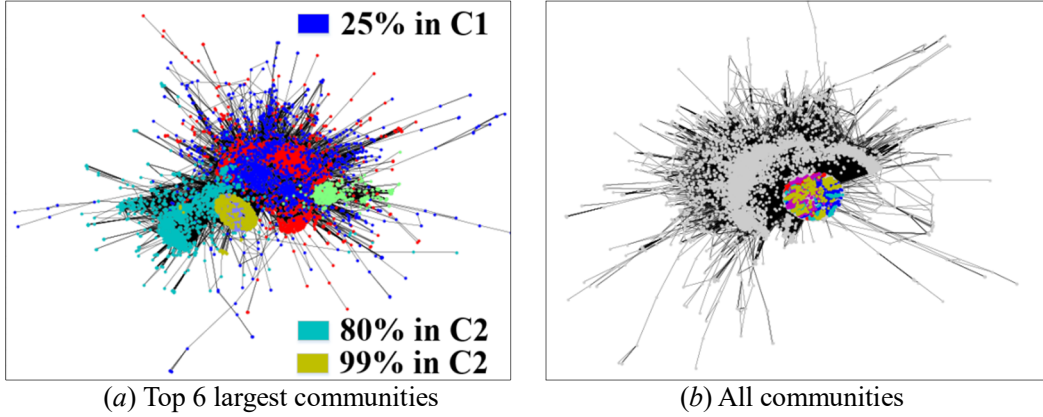


Fig. 11. Visualization of communities in a sampled subgraph of the web-Stanford network, where the subgraph was obtained by **RWR** with $R = 10\%$. (a) Top 6 largest communities, in which 25% of blue nodes are in C1, 80% of cyan nodes and 99% of yellow nodes are in C2. **Please note that C3 and C4 are lost.** (b) All communities, in which top 10 largest communities are marked as white, and other small communities are marked in color.

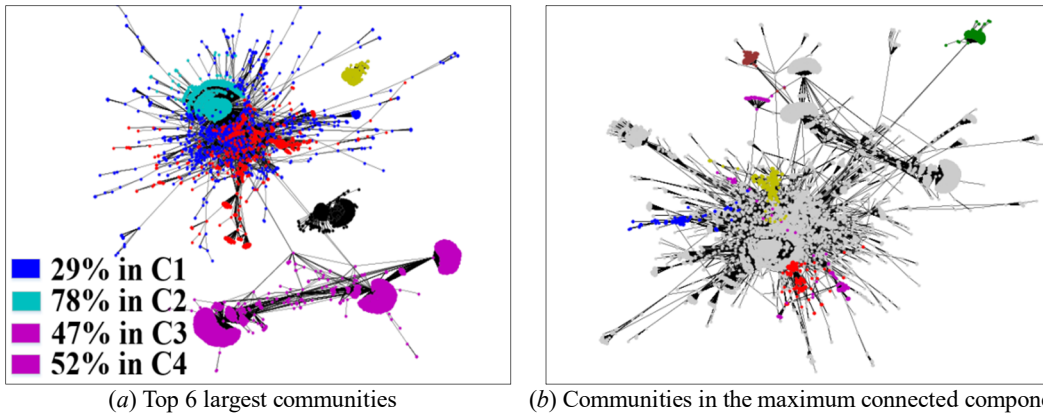


Fig. 12. Visualization of communities in a sampled subgraph of the web-Stanford network, where the subgraph was obtained by **RD** with $R = 10\%$. (a) Top 6 largest communities, in which 29% of blue nodes are in C1, 78% of cyan nodes are in C2, 47% of magenta nodes are in C3, and 52% of magenta nodes are in C4. (b) Communities in the maximum connected component, in which top 10 largest communities are marked as white, and other small communities are marked in color. **Please note that (a) is a disconnected graph**, where yellow is related to an isolated community.

In addition, Figs. 8(b) to 12(b) exhibit the global visualization. Specifically, we can observe that Fig. 8(b) captures more small and remote communities that are marked in color, which further validates the advantages of the double-layer sampling strategy adopted by SLSR.

6.3.4 Time efficiency of the traversal-based samplings

The sampling methods SLSR, FF, CNARW, RWR and RD run on another computer with Intel Core i7-8550U CPU 1.80 GHz Memory 20 G. The time comparisons of the sampling methods are listed in Table 9, which shows that SLSR maintains high time efficiency of unknown graph samplings. The running time of SLSR depends on the bisection method and the periphery sampling in Section 5. Specifically, the periphery sampling corresponds to the chosen T_s sampling, and the time

complexity of the bisection method is restricted by $\|V_{sub}^{per}\| \times \log_2 100$ where $\|V_{sub}^{per}\|$ denotes the number of sampled periphery nodes.

Table 9. Comparison of running time (Seconds) of SLSR and related methods that sample the original networks in Table 3 with given sampling rates R .

Sampling methods	Original networks and corresponding sampling rates				
	ego-Twitter	loc-Gowalla	com-DBLP	web-Stanford	com-Youtube
	$R = 5\%$	$R = 5\%$	$R = 10\%$	$R = 10\%$	$R = 5\%$
SLSR	09 s	21 s	299 s	063 s	160 s
FF	05 s	18 s	096 s	088 s	215 s
CNARW	32 s	33 s	032 s	306 s	243 s
RWR	07 s	08 s	010 s	105 s	040 s
RD	01 s	03 s	003 s	016 s	017 s

6.3.5 Analysis of the random node sampling

In contrast to other traversal-based samplings, SLSR needs an additional AD and DT evaluation based on random node sampling. Please note that the AD of the subgraph induced by the nodes randomly chosen by the RN sampling^[5] is much smaller than the evaluated AD because of loss of many important high-degree nodes in the subgraph. However, the high-degree nodes are not lost in the neighbor sets $N_{org}(v)$ of the randomly chosen nodes, because $N_{org}(v)$ is defined as the set of the neighbor nodes of the chosen node v in the original graph that contains the high-degree nodes, and the dense connections between the core and periphery nodes, shown in Table 2, ensure that the high-degree nodes are not lost in the neighbor sets $N_{org}(v)$. Therefore, the random node sampling is only suitable for the evaluation of AD and DT, and cannot directly output a sampled subgraph capturing the degree property or other important properties^[5], as shown in Fig. 13.

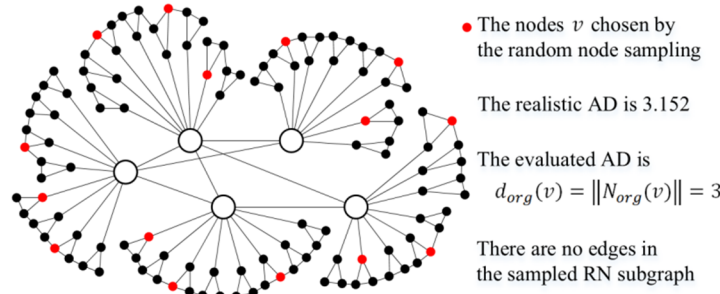


Fig. 13. The random node sampling on a core-periphery graph, in which $N_{org}(v)$ is defined in the original graph, not in the RN subgraph, and can be obtained by the traversal-based samplings.

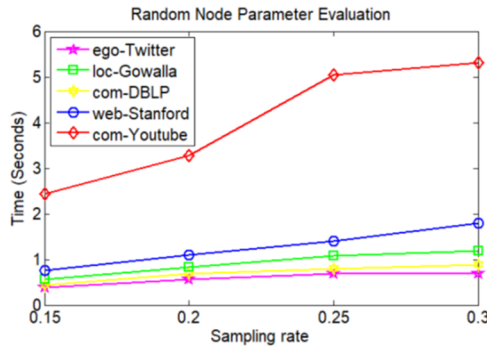


Fig. 14. Time (Seconds) vs. sampling rate R of the random node sampling for the evaluation of AD and DT, on the five original networks described in Table 3.

The nodes in the original network G_{org} are independently chosen by the random node sampling, that is, the complex topological correlation between the nodes is ignored, which results in a very high time efficiency of the random node sampling, as shown in Fig. 14, and the loss of many important properties (including the degree property) in the sampled RN subgraph^[5].

7 Conclusions

This paper proposes a double-layer sampling framework for unknown large networks restricted by low sampling rates. The framework can effectively avoid the excessive preference for high-degree core nodes and realize a balance sampling between core and periphery. The proposed sampling SLSR starts by a random node sampling to evaluate the AD and DT of original networks, and then implements a periphery sampling and a bisection method under the guidance of the evaluated AD and DT. SLSR is simple that results in a fast sampling on large networks with more than one million nodes, but it can preserve many critical structures except for degree, including assortativity, path length, clustering, graph spectrum, centrality and communities.

References

- [1] H Zeng, H Zhou, A Srivastava, R Kannan, V Prasanna. Graphsaint: Graph sampling based inductive learning method, *In Eighth International Conference on Learning Representations*, Virtual Conference, Formerly Addis Ababa ETHIOPIA, April 26-30, 2020.
- [2] T Zheng, L Wang. Large graph sampling algorithm for frequent subgraph mining. *IEEE Access*, 2021, 9: 88970-88980.
- [3] P Jiang, Y Wei, J Su, R Wang, B Wu. SampleMine: A framework for applying random sampling to subgraph pattern mining through loop perforation. *In International Conference on Parallel Architectures and Compilation Techniques*, Chicago, USA, 2022.
- [4] M Zhu, W Chen, Y Hu, Y Hou, L Liu, K Zhang. DRGraph: An efficient graph layout algorithm for large-scale graphs by dimensionality reduction, *IEEE Transactions on Visualization and Computer Graphics*, 2021, 27(2): 1666-1676.
- [5] J Leskovec, C Faloutsos, Sampling from large graphs, *In Proceedings of the 12th ACM SIGKDD International Conference on Knowledge Discovery and Data Mining*, 2006: 631-636.
- [6] S Hong, S Lu. Graph sampling methods for big complex networks integrating centrality, k -core, and spectral sparsification. *In The 35th ACM/SIGAPP Symposium on Applied Computing*, New York, USA, 2020.
- [7] Z Zhang, P Cui, W Zhu. Deep learning on graphs: A survey. *IEEE Transactions on Knowledge and Data Engineering*, 2020, 34: 249-270.
- [8] N Martin, P Frasca, C Canudas-de-Wit. Large-scale network reduction towards scale-free structure. *IEEE Transactions on Network Science and Engineering*, 2018, 6: 711-723.
- [9] B Jiao, X Lu, J Xia, B B Gupta, L Bao, Q Zhou. Hierarchical sampling for the visualization of large scale-free graphs. *IEEE Transactions on Visualization and Computer Graphics*, 2022, DOI: 10.1109/TVCG.2022.3201567.
- [10] C Lee, X Xu, D Eun. Beyond random walk and metropolis-hastings samplers: Why you should not backtrack for unbiased graph sampling. *In Proceedings of the 2012 ACM SIGMETRICS*, 2012.

- [11] J Lu, D Li. Sampling online social networks by random walk. *In Proceedings of the First ACM international workshop on hot topics on interdisciplinary social networks research*, 2012.
- [12] X Zhang, T Martin, M E J Newman. Identification of core-periphery structure in networks. *Physical Review E*, 2015, 91: 032803.
- [13] P Rombach, M A Porter, J H Fowler, P J Mucha. Core-periphery structure in networks (revisited). *SIAM review*, 2017, 59(3): 619-646.
- [14] F Tudisco, D J Higham. A nonlinear spectral method for core-periphery detection in networks. *SIAM Journal on Mathematics of Data Science*, 2019, 1(2): 269-292.
- [15] P Csermely, A London, L Wu, B Uzzi. Structure and dynamics of core/periphery networks. *Journal of Complex Networks*, 2013, 1(2): 93-123.
- [16] O Ben-Eliezer, T Eden, J Oren, D Fotakis. Sampling multiple nodes in large networks: Beyond random walks. *In Proceedings of the Fifteenth ACM International Conference on Web Search and Data Mining*, 2022: 37-47.
- [17] J Leskovec, J Kleinberg, C Faloutsos. Graphs over time: Densification law, shrinking diameters and possible explanations. *In Proceedings of the 11th ACM SIGKDD International Conference on Knowledge Discovery in Data Mining*, 2005: 177-187.
- [18] Y Li, Z Wu, S Lin, H Xie, M Lv, Y Xu, J C S Lui. Walking with perception: Efficient random walk sampling via common neighbor awareness. *IEEE 35th International Conference on Data Engineering*, 2019: 962-973.
- [19] E Voudigari, N Salamanos, T Papageorgiou, E J Yannakoudakis. Rank degree: An efficient algorithm for graph sampling. *In Proceedings of the IEEE/ACM International Conference on Advances in Social Networks Analysis and Mining*, 2016: 120-129.
- [20] A S Maiya, T Y Berger-Wolf. Sampling community structure. *In Proceedings of the 19th International Conference on World Wide Web*, 2010: 701-710.
- [21] A Rezvanian, M R Meybodi. Sampling social networks using shortest paths. *Physica A: Statistical Mechanics and its Applications*, 2015, 424: 254-268.
- [22] L Zhang, H Jiang, F Wang, D Feng. DRaWS: A dual random-walk based sampling method to efficiently estimate distributions of degree and clique size over social networks. *Knowledge-Based Systems*, 2020, 198: 105891.
- [23] N K Ahmed, J Neville, R Kompella. Network sampling: From static to streaming graphs. *ACM Transactions on Knowledge Discovery from Data*, 2013, 8: 1-56.
- [24] A Zakrzewska, D A Bader. Streaming graph sampling with size restrictions. *In Proceedings of the IEEE/ACM International Conference on Advances in Social Networks Analysis and Mining*, 2017: 282-290.
- [25] A L Barabasi, R Albert. Emergence of scaling in random networks. *Science*, 1999, 286(5439): 509-512.
- [26] S Kojaku, N Masuda. Core-periphery structure requires something else in the network. *New Journal of Physics*, 2018, 20(4): 043012.
- [27] Stanford Large Network Dataset Collection, <http://snap.stanford.edu/data/>, accessed 2023.
- [28] J Winick, S Jamin. Inet-3.0: Internet topology generator. *Technical Report CSE-TR-456-02, University of Michigan*, 2002: 456-02.
- [29] D Antonakaki, P Fragopoulou, S Ioannidis. A survey of Twitter research: Data model, graph structure, sentiment analysis and attacks. *Expert Systems with Applications*, 2021, 164: 114006.

- [30] M A Manouchehri, M S Helfroush, H Danyali. Temporal rumor blocking in online social networks: A sampling-based approach. *IEEE Transactions on Systems, Man, and Cybernetics: Systems*, 2021, 52: 4578-4588.
- [31] H Haddadi, M Rio, G Lannaccone, A Moore, R Mortier. Network topologies: Inference, modeling, and generation. *IEEE Communications Surveys & Tutorials*, 2008, 10: 48-69.
- [32] A Rezvanian, M R Meybodi. Sampling algorithms for stochastic graphs: A learning automata approach. *Knowledge-Based Systems*, 2017, 127(1): 126-144.
- [33] T Wang, Y Chen, Z Zhang, T Xu, L Jin, P Hui, et al. Understanding graph sampling algorithms for social network analysis. In *31st International Conference on Distributed Computing Systems Workshops*, 2011: 123-128.
- [34] M E Newman. Mixing patterns in networks. *Physical review E*, 2003, 67(2): 026126.
- [35] M I Yousuf, S Kim. Guided sampling for large graphs. *Data mining and knowledge discovery*, 2020, 34(4): 905-948.
- [36] S H Lee, P J Kim, H Jeong. Statistical properties of sampled networks. *Physical review E*, 2006, 73: 016102.
- [37] B Jiao, Y Nie, J Shi, C Huang, Y Zhou, J Du, R Guo, Y Tao. Scaling of weighted spectral distribution in deterministic scale-free networks. *Physica A*, 2016, 451: 632-645.
- [38] D Fay, H Haddadi, A Thomason, A W Moore, R Mortier, et al. Weighted spectral distribution for internet topology analysis: theory and applications. *IEEE/ACM Transactions on networking*, 2009, 18(1): 164-176.
- [39] B Jiao, J Shi, W Zhang, L Xing. Graph sampling for internet topologies using normalized Laplacian spectral features. *Information Sciences*, 2019, 481: 574-603.
- [40] B Jiao, Y Nie, J Shi, G Lu, Y Zhou, J Du. Accurately and quickly calculating the weighted spectral distribution. *Telecommunication Systems*, 2016, 62: 231-243.
- [41] B Jiao, Y Zhou, J Du, C Huang, Z Lu, Y Liu. Study on the stability of the topology interactive growth mechanism using graph spectra. *IET Communications*, 2014, 8(16): 2845-2857.
- [42] B Wei, Y Deng. A cluster-growing dimension of complex networks: From the view of node closeness centrality. *Physica A: Statistical Mechanics and its Applications*, 2019, 522: 80-87.
- [43] C Fan, L Zeng, Y Ding, M Chen, Y Sun, Z Liu. Learning to identify high betweenness centrality nodes from scratch: A novel graph neural network approach. In *Proceedings of the 28th ACM International Conference on Information and Knowledge Management*, 2019: 559-568.
- [44] P Thai, M T Thai, T Vu, T Dinh. Saphyra: A learning theory approach to ranking nodes in large networks. In *2022 IEEE 38th International Conference on Data Engineering*, 2022: 54-67.
- [45] I B El Kouni, W Karoui, L B Romdhane. Node importance based label propagation algorithm for overlapping community detection in networks. *Expert Systems with Applications*, 2020, 162: 113020.
- [46] P De Meo, E Ferrara, G Fiumara, A Provetti. Generalized louvain method for community detection in large networks. In *2011 11th international conference on intelligent systems design and applications*, 2011: 88-93.
- [47] S Zellmann, M Weier, I Wald. Accelerating force-directed graph drawing with RT cores. In *2020 IEEE Visualization Conference*, 2020: 96-100.